Semiconductor Physics, Quantum Electronics & Optoelectronics, 2022. V. 25, No 4. P. 355-361.

Semiconductor physics

Redistribution of centers responsible for radiative recombination in SiC/por-SiC and SiC/por-SiC/Er_2O_3 structures under nonthermal action of microwave radiation

O.B. Okhrimenko*, Yu.Yu. Bacherikov, O.F. Kolomys, V.V. Strelchuk, R.V. Konakova

V. Lashkaryov Institute of Semiconductor Physics, NAS of Ukraine,
41, prosp. Nauky, 03680 Kyiv, Ukraine
**E-mail: olga@isp.kiev.ua*

Abstract. In this work, the authors have considered the effect of short-term nonthermal action of microwave radiation on the photoluminescent characteristics of SiC/por-SiC/Er_2O_3 and SiC/por-SiC structures. The analysis of photoluminescence spectra of these structures, which are excited by radiation with an energy lower than the band gap in the 4H-SiC crystalline substrate, has shown that short-term action of microwave radiation leads to redistribution of radiative recombination centers, which is caused by surface states in the por-SiC layer.

Keywords: nonthermal microwave action, buffer porous layer, photoluminescence, Raman scattering, silicon carbide.

https://doi.org/10.15407/spqeo25.04.355
PACS 81.07.-b, 85.40.Sz

Manuscript received 16.09.22; revised version received 14.10.22; accepted for publication 14.12.22; published online 22.12.22.

1. Introduction

In the modern microelectronic industry, silicon carbide is considered as a promising alternative to silicon, especially in high-power, high-temperature, and high-frequency devices [1–4]. The advantages of silicon carbide include high thermal, radiation and chemical resistance. This makes it possible to use silicon carbide as substrates for structures in electronic devices, namely: in microwave devices, UV photodiodes, LEDs [5]. The most common structures used in electronics are the metal-insulator-semiconductor (MIS) structures. Thin oxide films are most often used as dielectrics in these structures. In this case, the mismatch between parameters of the silicon carbide crystal lattice and those of the oxide film has a significant effect on the characteristics of the semiconductor/insulator interface in the MIS structure. At the same time, the use of additional porous silicon carbide buffer layers in the SiC/por-SiC/oxide structures enables to modify the interface parameters, which expands the range of application of silicon carbide-based structures. In this case, quality of SiC/por-SiC/oxide structures containing porous silicon carbide buffer layers, their stability and suitability to be used in extreme operation conditions will be largely defined by both the characteristics of the semiconductor substrate and quality of the dielectrics and the dielectric/porous layer interface.

In addition to being used as a buffer layer, porous silicon carbide is also promising for light emitting diodes, photodetectors, sensors, and substrates for epitaxial deposition [6–8]. In addition, as shown in [6, 9–11] one can use the possibility of creating the fluorescent white LEDs based on SiC and por-SiC. The developed por-SiC surface and presence of a large number of surface bonds that are formed during etching can serve as adsorption centers for various molecules of analytes or traps (sticking centers), which allows one to consider por-SiC as a promising material for creating the sensor devices based on it [5, 12–15].

To reduce the concentration of defect states at the oxide-semiconductor interface, additional external treatments are often used, namely: thermal annealing, γ-irradiation and microwave irradiation. For example, the effect of an increase in the transmission coefficient for the SiC/SiO_2 and SiC/TiO_2(Gd_2O_3, Er_2O_3) structures after microwave action was observed in [16, 17]. In [18], to explain the changes in the optical properties of these structures, a model for the nonthermal action of microwave radiation on oxide film/semiconductor structures was proposed. According to this model, the microwave treatment increases the migration capability of dislocations, which, in its turn, leads to redistribution of emission and absorption centers in the oxide film/silicon carbide structures.

In this work, we studied the effect of short-term microwave action on redistribution of impurity-defect states in the 4H-SiC/por-SiC and 4H-SiC/por-SiC/Er_2O_3 structures.

2. Samples and experimental procedure

A porous surface in silicon carbide (for which the initial material was the 4H-SiC polytype) was produced using electrochemical etching in the solution HF:C_2H_5OH = 1:1 at the current density 10 mA/cm^2 and etching time 10 min. Then, the material was treated in a KOH melt at the temperature 550 °C to uncover the pores. At the following stage, an erbium film was deposited on the surface of porous silicon carbide by using the method of thermal sputtering. The structures of porous SiC with a deposited erbium layer were annealed in vacuum at the temperature 800 °C for 8 min. After that, in the rapid thermal annealing (RTA) mode in dry oxygen atmosphere at the temperature 400 °C a thin oxide film of Er_2O_3 was formed on the por-SiC surface. The RTA periods were 1, 3 and 5 s. The thickness of the prepared oxide layers, being determined using the Auger spectroscopy [19], was approximately 100 nm. An increase in the RTA time was accompanied by an increase in the fraction of the Er oxide film with a stoichiometric composition relative to the underoxidized metal layer [19].

Microwave treatment was carried out in the magnetron operation chamber with the frequency f = 2.45 GHz and specific power of ~0.04 W/cm^3. The total microwave action time was 5 s.

The photoluminescence (PL) and micro-Raman spectra of the samples were obtained in the backscattering geometry by using a Horiba Jobin Yvon T64000 spectrometer with a confocal microscope and a cooled CCD detector. In the Raman studies, the laser beam was focused into the spot < 1 μm in diameter. The accuracy of determining the frequency position of phonon lines was 0.15 cm^{-1}.

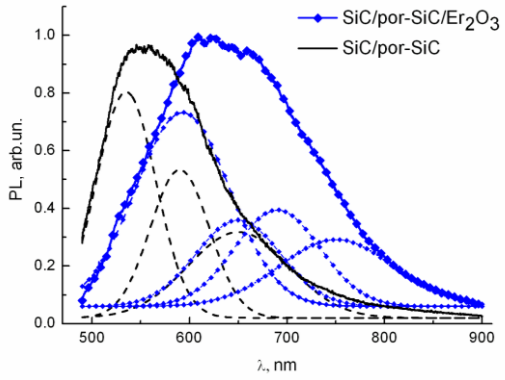

Fig. 1. Typical normalized PL spectra (λ_{exc} = 488 nm, $h\nu_{exc}$ = 2.5 eV < E_g (4H-SiC) = 3.2 eV (solid line) and decomposition into contour components (dashed line) for the initial SiC/por-SiC (*1*) and SiC/por-SiC/Er_2O_3 (*2*) structures.

To register PL associated directly with radiative recombination in the por-SiC or por-SiC/Er_2O_3 layer, the radiation of an Ar-Kr laser with λ_{exc} = 488.0 nm was chosen as the exciting one. This choice of photoluminescence exciting radiation for the SiC/por-SiC and SiC/por-SiC/Er_2O_3 structures was caused by the fact that the energy corresponding to λ_{exc} = 488 nm is $h\nu_{exc}$ = 2.5 eV, which is less than the band gap energy of crystalline 4H-SiC (E_g = 3.23 eV, which corresponds to λ = 384 nm). Raman spectra were also excited by Ar-Kr laser radiation (λ_{exc} = 488.0 nm). All optical measurements were carried out at room temperature.

3. Experimental results and discussion

Fig. 1 shows the typical PL spectra for the initial SiC/por-SiC and SiC/por-SiC/Er_2O_3 structures, which are normalized to the maximum. As shown in [20, 21], appearance of luminescence excited with the light energy less than the band gap one in the initial crystalline silicon carbide polytype 6H-SiC (E_g =3.02 eV corresponds to λ = 413 nm) or 4H-SiC (E_g = 3.23 eV corresponds to λ = 384 nm) is a characteristic feature of luminescence in por-SiC. Luminescence is not observed for the 4H-SiC crystalline substrate at λ_{exc} = 488 nm. Since PL was excited by radiation with λ_{exc} = 488 nm, all the features of the PL spectra shown in Fig. 1 are caused by the por-SiC or por-SiC/Er_2O_3 layer. The shape of the PL spectra of the SiC/por-SiC/Er_2O_3 structures at λ_{exc} = 488 nm is practically independent of the RTA time.

As noted earlier, the distinctive feature of por-SiC is the presence of photoluminescence even in the case, when the energy of the exciting radiation is less than the energy of the band gap of the initial crystalline material of the 4H-SiC and 6H-SiC substrate, E_g = 3.23 eV and 3.02 eV, respectively [20, 21]. Herewith, the PL spectra of por-SiC for the 4H-SiC, 6H-SiC (α-SiC), and 3C-SiC (β-SiC) polytypes are almost the same [5, 20, 22]. In the literature, these features of the PL spectrum of por-SiC are associated either with the manifestation of quantum confinement [23–25] or with the appearance of crystallites of the 3C-SiC cubic phase in the porous layer [26], or with impurity-defect states that arise on the surface of por-SiC during its processing, as well as due to the products of chemical reactions during etching [6, 20, 23–25, 27–35]. Formation of crystallites of the cubic phase silicon carbide in the samples of porous silicon carbide grown on 4H-SiC or 6H-SiC substrates is explained by the fact that, as a result of electrochemical etching, the interlayer bonds in the structure of the 4H-SiC crystal are broken, and thin layers consisting of crystallites of 3C-SiC cubic phase are formed. In [21], the absorption and photoluminescence spectra of porous silicon carbide prepared using anodic etching were studied at different wavelengths of exciting radiation. According to the data of [21], the unchangeable position of the absorption edge of por-SiC with respect to the absorption edge of the crystalline substrate indicates the absence of additional thin layers in por-SiC formed from the cubic phase of SiC. Therefore, the appearance of PL

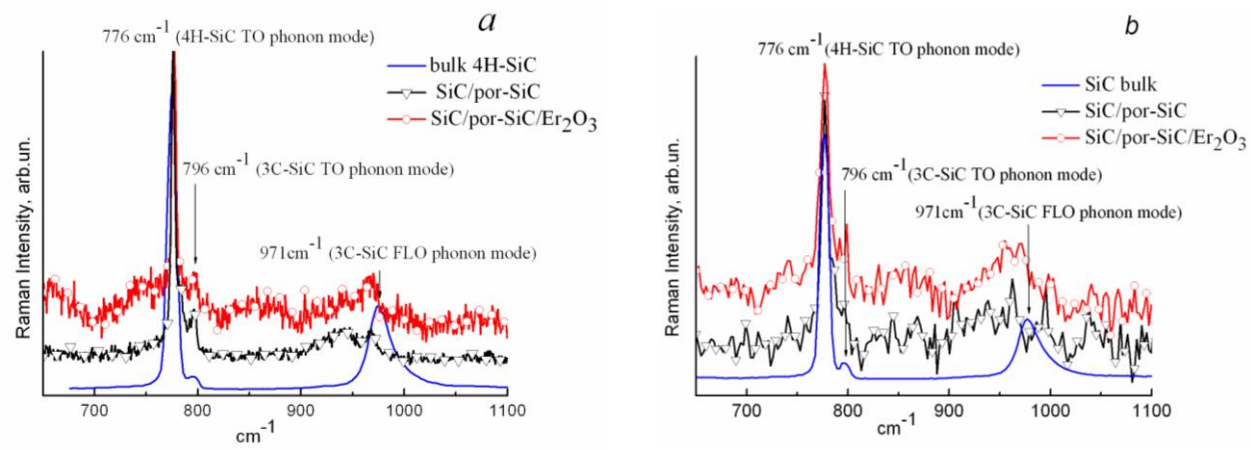

Fig. 2. Raman spectra of the structures SiC, SiC/por SiC and SiC/por SiC/Er_2O_3 before (a) and after (b) microwave treatment (λ_{exc} = 488 nm).

in por-SiC at the excitation energy $h\nu_{exc} \le E_g$ is associated with appearance of emission centers formed by impurity atoms and surface defects that appear during anodic etching of the SiC crystalline substrate and subsequent processing that opens the pores. Formation of complex compounds (namely, oxides and siloxenes) and Si–H or C–H bonds, as well as C–N (nitrogen is an uncontrolled impurity in SiC) in the por-SiC layer occurs due to the violation of Si–C bonds during etching of crystalline silicon carbide [29, 36–38]. At the same time, it is also impossible to exclude the presence of insignificant amounts of the 3C-SiC phase in por-SiC as structural defects, such as stacking faults.

As can be seen from Fig. 1, the PL bands have a large half-width and consist of several individual PL bands with $\lambda_{max} \approx$ 535, 590 and 650 nm. According to [39], the band with $\lambda_{max} \approx$ 535 nm can be associated with carbon fluorooxide (CFO) that can be formed during electrochemical etching of a SiC crystalline substrate in the HF:C_2H_5OH solution. The band with $\lambda_{max} \approx$ 590 nm is probably caused by the presence of microcrystallites of cubic silicon carbide 3C-SiC in por-SiC [40, 41]. The origin of the low-energy PL peak with $\lambda_{max} \approx$ 650 nm can be explained by radiative recombination in some localized states (shallow traps) [27] or in donor-acceptor-pairs (DAP) [28].

When the Er_2O_3 oxide film is deposited onto por-SiC, a change in the shape of PL spectrum is observed (Fig. 1). Thus, deposition of the Er_2O_3 oxide film leads to the quenching of the band with $\lambda_{max} \approx$ 535 nm and the appearance of additional bands with $\lambda_{max} \approx$ 690 nm and $\lambda_{max} \approx$ 750 nm, the intensity of the band with $\lambda_{max} \approx$ 590 nm increases, while the intensity of band with $\lambda_{max} \approx$ 650 nm remains practically unchanged. A similar change in the PL spectra was noted in [6] when studying the passivating Al_2O_3 or TiO_2 films on the surface of porous silicon carbide. The appearance of additional bands with $\lambda_{max} \approx$ 690 nm and $\lambda_{max} \approx$ 750 nm in the PL spectrum during deposition of an oxide film can be explained by additional oxidation of the porous surface inherent to silicon carbide [6]. Since deposition of oxide layers is accompanied by heat treatment of the entire structure, excess unreacted oxygen atoms localized in the pores of por-SiC can additionally oxidize the surface of por-SiC [6]. Therefore, the appearance of additional bands and redistribution of intensity in other bands in the PL spectrum of SiC/por-SiC/Er_2O_3 structure can be associated with radiative recombination in oxygen-related defects.

Additional information about the presence of the 3C-SiC phase in por-SiC as structural defects was obtained from the Raman spectra. Figs 2a and 2b show the Raman spectra of the 4H-SiC substrate, SiC/por-SiC, SiC/por-SiC/Er_2O_3 structures, normalized to the intensity of 776 cm^{-1} line corresponding to 4H-SiC TO phonon mode [42], before and after microwave treatment. In the Raman spectra of the SiC/por-SiC and SiC/por-SiC/Er_2O_3 structures, the luminescent background has been subtracted for the ease of comparison. As can be seen from Fig. 2, both in the 4H-SiC substrate and in the SiC/por-SiC and SiC/por-SiC/Er_2O_3 structures, along with the 776 cm^{-1} line, there are 796 cm^{-1} lines (3C-SiC TO phonon mode [42]), 965 cm^{-1} (4H-SiC FLO phonon mode [42]), 971 cm^{-1} (3C-SiC FLO phonon mode [42]), and 971 cm^{-1} (3C-SiC FLO phonon mode [42]). In so doing, the intensity ratio of these lines remains almost constant for 4H-SiC, SiC/por-SiC, and SiC/por-SiC/Er_2O_3 (Fig. 2a). This fact confirms the conclusion that appearance of PL in por-SiC at the energy of exciting radiation $h\nu_{exc} \le E_g$ (4H-SiC) is not associated with formation of an additional layer of the 3C-SiC cubic phase in the por-SiC layer. At the same time, individual centers of por-SiC radiative luminescence can be associated with structural defects caused by stacking faults, *i.e.* clusters of the 3C-SiC cubic phase.

As can be seen from Fig. 2b, the microwave treatment also has no significant effect on the intensity ratio of the Raman lines corresponding to the 4H-SiC and 3C-SiC polytypes. Thus, being based on the Raman data, we can conclude that microwave treatment does not lead to a significant change in the ratio of 4H-SiC/3C-SiC crystalline phases in the structures under study.

Fig. 3 shows typical normalized PL spectra upon PL excitation by radiation with $h\nu_{exc} = 2.5$ eV < E_g (4H-SiC, 3.23 eV) and decomposition of the PL spectra into contour components for the SiC/por-SiC and SiC/por-SiC/Er_2O_3 structures before and after microwave action. It should be noted that the PL spectra of the SiC/por-SiC/Er_2O_3 structures, both initial ones and those after microwave action, are practically independent of the RTA time. As can be seen from Fig. 3, the PL spectrum for the SiC/por-SiC and SiC/por-SiC/Er_2O_3 structures is a wide band that has a complex character and consists of several overlapping PL bands caused by different PL centers, the concentration of which varies depending on microwave processing.

As can be seen from Fig. 3a, the microwave treatment of SiC/por-SiC structure leads to broadening of the integrated PL spectrum and a slight shift of the maximum of integral PL band to the long-wave side, which is caused by appearance of a broad additional PL band with $\lambda_{max} \approx 690$ nm.

At the same time, for the SiC/por-SiC/Er_2O_3 structure (Fig. 3b), after microwave treatment, there is a change in the intensities of individual bands composing the integral PL band of the SiC/por-SiC/Er_2O_3 structure and quenching of the band with the peak $\lambda_{max} \approx 750$ nm. In this case, the intensity and half-width of the band with the peak $\lambda_{max} \approx 590$ nm remain practically unchanged. As a result, we observed a short-wave shift of the peak of integral PL band for the SiC/por-SiC/Er_2O_3 structures after microwave treatment and a decrease in the half-width of integral PL spectrum (Fig. 3b).

As can be seen from Fig. 3c, microwave treatment leads to the appearance of a band with $\lambda_{max} \approx 535$ nm in the PL spectrum of SiC/por-SiC/Er_2O_3 structure, and a weak band with $\lambda_{max} \approx 690$ nm appears in the PL spectrum of SiC/por-SiC structure. In this case, the overlap region of the PL spectra of the SiC/por-SiC and SiC/por-SiC/Er_2O_3 structures significantly increases in comparison with the overlap region of the PL spectra of these structures in the initial state (Figs 1, 3c).

In [18], the change in the temperature of the silicon carbide crystalline substrate/oxide film structure was considered as a result of microwave irradiation with the frequency $f = 2.45$ GHz and the power density ~0.04 W/cm^3. The estimates were made under the assumption that the microwave radiation was completely absorbed by the semiconductor substrate. It was shown [18] that during the irradiation time 1 s, the temperature of a sample with geometric dimensions ~0.5×0.5×0.04 cm (which corresponds to the geometric dimensions of the samples studied in this work) can change by $\Delta T = 0.02$ deg. According to [43], the rate of microwave heating of por-SiC is about 4 times lower than that of crystalline SiC. Therefore, a short-term microwave action on the 4H-SiC/por-SiC and 4H-SiC/ por-SiC/Er_2O_3 structures can be considered as nonthermal. Thus, it is impossible to relate the observed changes in the PL and Raman spectra with the temperature effect accompanying the microwave treatment.

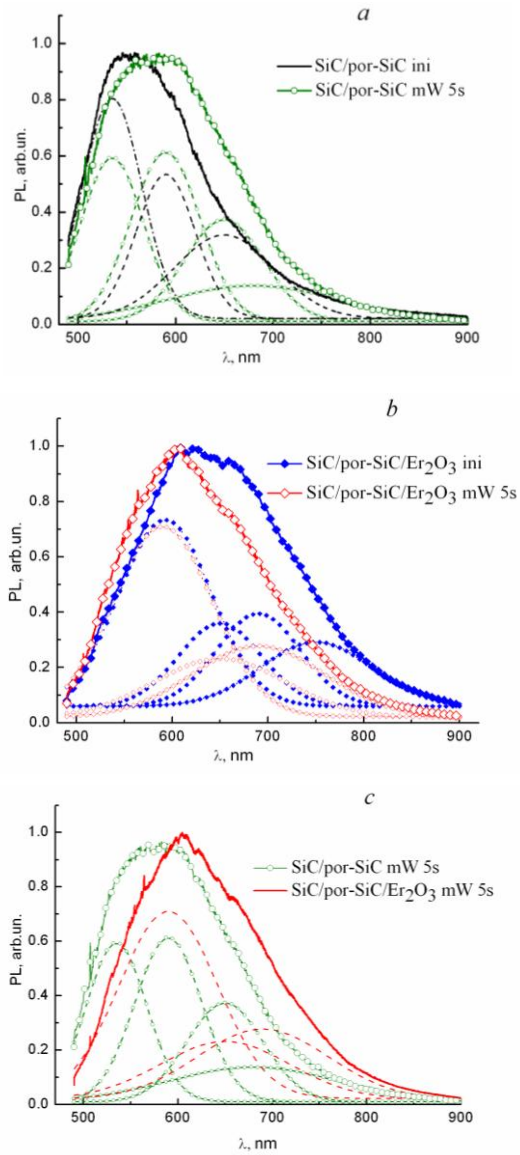

Fig. 3. Typical normalized PL spectra (λ_{exc} = 488 nm, $h\nu_{exc} = 2.5$ eV < E_g (4H-SiC, 3.23 eV) and decomposition into contour components for the structures: (a) SiC/por-SiC, (b) SiC/por-SiC/Er_2O_3, (c) SiC/por-SiC and SiC/por-SiC/Er_2O_3 before and after microwave action.

Changes in the PL spectra of SiC/por-SiC, SiC/por-SiC/Er_2O_3 structures after microwave treatment (Fig. 3) are probably caused by the fact that microwave action leads to dislocation movement, similar to that observed under ultrasound action [44]. In its turn, the movement of dislocations under the microwave action can lead to a redistribution of dopants and defects in the SiC/por-SiC and por-SiC/Er_2O_3 structures. This results in a change in the nature of the interimpurity interaction between luminescence centers [45, 46] and a change in the symmetry of the nearest environment of silicon carbide impurity atoms. In addition, according to [47], microwave radiation can serve as a catalyst for chemical reactions, which in its turn can lead to a change in the concentration of Si–H, C–H or C–N bonds in the por-SiC buffer layer.

4. Conclusions

Thus, nonthermal microwave radiation action on the SiC/por SiC and SiC/por-SiC/Er_2O_3 structures leads to redistribution of radiative recombination centers in these structures. This redistribution of PL centers may be associated with the simultaneous action of several factors. Under microwave radiation action, dislocations detach from the stopper, which leads to their migration in the field of mechanical strains of the crystal lattice, and as a result, to a change in both the number and localization of dislocations in the structure and, accordingly, to a redistribution of recombination centers. Also, microwave action can lead to a change in the concentration of Si–H, C–H or C–N bonds in the buffer layer of por-SiC, as well as to appearance of additional PL centers due to additional oxidation of silicon in the buffer porous layer of the SiC/por-SiC/Er_2O_3 structure.

References

1. Li F., Roccaforte F., Greco G. *et al.* Status and prospects of cubic silicon carbide power electronics device technology. *Materials* (Basel). 2021. **14**. P. 5831. https://doi.org/10.3390/ma14195831.
2. Matsunami H. Fundamental research on semiconductor SiC and its applications to power electronics. *Proc. Jpn. Acad. Ser. B: Phys. Biol. Sci*. 2020. **96**. P. 235–254. https://doi.org/10.2183/pjab.96.018.
3. Le H.T., Haque R.I., Ouyang Z. *et al.* MEMS inductor fabrication and emerging applications in power electronics and neurotechnologies. *Microsyst. Nanoeng.* 2021. **7**. P. 59. https://doi.org/10.1038/s41378-021-00275-w.
4. Papanasam E., Prashanth Kumar B., Chanthini B. *et al.* A comprehensive review of recent progress, prospect and challenges of silicon carbide and its applications. *Silicon.* 2022. https://doi.org/10.1007/s12633-022-01998-9.
5. Rashid M., Horrocks B.R., Healy N. *et al*. Optical properties of mesoporous 4H-SiC prepared by anodic electrochemical etching. *J. Appl. Phys.* 2016. **120**. P. 194303. https://doi.org/10.1063/1.4968172.
6. Lu W., Ou Y., Petersen P.M. *et al*. Fabrication and surface passivation of porous 6H-SiC by atomic layer deposited films. *Opt. Soc. Amer*. 2016. **6**. P. 1956–1963. https://doi.org/10.1364/OME.6.001956.
7. Monaico E., Tiginyanu I. and Ursaki V. Porous semiconductor compounds. *Semicond. Sci. Technol.* 2020. **35**. P. 103001. https://doi.org/10.1088/1361-6641/ab9477.
8. Naderi N., Hashim M.R. Visible-blind ultraviolet photodetectors on porous silicon carbide substrates. *Mater. Res. Bull.* 2013. **48**. P. 2406–2408. https://doi.org/10.1016/j.materresbull.2013.02.078.
9. Nagasawa F., Takamura M., Sekiguchi H. *et al.* Prominent luminescence of silicon-vacancy defects created in bulk silicon carbide *p-n* junction diodes. *Sci. Rep*. 2021. **11**. P. 1497. https://doi.org/10.1038/s41598-021-81116-8.
10. Ou H., Ou Y., Argyraki A. *et al*. Advances in wide bandgap SiC for optoelectronics. *Eur. Phys. J. B: Condensed Matter Physics*. 2014. **87**. P. 58. https://doi.org/10.1140/epjb/e2014-41100-0.
11. Zhang F. SiC: An excellent platform for single-photon detection and emission. *Sci. China Phys. Mech. Astron.* 2022. **65**. P. 107331. https://doi.org/10.1007/s11433-022-1941-5.
12. Naderi N., Moghaddam M. Ultra-sensitive UV sensors based on porous silicon carbide thin films on silicon substrate. *Ceramics Int*. 2020. **46**. P. 13821–13826. https://doi.org/10.1016/j.ceramint.2020.02.173.
13. Anwar M.S., Bukhari S.Z.A., Ha J.-H. *et al.* Controlling the electrical resistivity of porous silicon carbide ceramics and their applications: A review. *Appl. Ceram. Technol*. 2022. **19**. P. 1814–1840. https://doi.org/10.1111/ijac.14034.
14. Raju P., Li Q. Review – Semiconductor materials and devices for gas sensors. *J. Electrochem. Soc.* 2022. **169**. P. 057518. https://iopscience.iop.org/article/10.1149/1945-7111/ac6e0a/pdf.
15. Kim K.S., Chung G.S., Al-Ghamdi A.A., Yakuphanoglu F. Hydrogen sensing characteristics of vertical type hydrogen sensors based on porous 3C-SiC with catalyst materials. *Microsyst. Technol*. 2013. **19**. P. 1221. https://doi.org/10.1007/s00542-012-1722-7.
16. Bacherikov Yu.Yu., Konakova R.V., Kocherov A.N. *et al*. Effect of microwave annealing on silicon dioxide/silicon carbide structures. *Tech. Phys*. 2003. **48**. P. 598–601. https://doi.org/10.1134/1.1576474.
17. Bacherikov Yu.Yu., Konakova R.V., Milenin V.V. *et al*. Changes in characteristics of gadolinium, titanium, and erbium oxide films on the SiC surface under microwave treatment. *Semiconductors*. 2008. **42**. P. 868–872. https://doi.org/10.1134/S1063782608070191.
18. Okhrimenko O.B. Phenomenological model of athermal interaction of microwave radiation with the structures wide-gap semiconductor – oxide film. *SPQEO*. 2015. **18**. No 4. P. 452–455. https://doi.org/10.15407/spqeo18.04.452.
19. Bacherikov Yu.Yu., Konakova R.V., Okhrimenko O.B. *et al*. Optical properties of thin erbium oxide films formed by rapid thermal annealing on SiC substrates with different structures. *SPQEO*. 2017. **20**, No 4. P. 465–469. https://doi.org/10.15407/spqeo20.04.465.
20. Konstantinov A.O., Henry A., Harris C.I. *et al*. Photoluminescence studies of porous silicon carbide. *Appl. Phys. Lett*. 1995. **66**. P. 2250–2252. https://doi.org/10.1063/1.113182.
21. Berezovska N.I., Bacherikov Yu.Yu., Konakova R.V. *et al.* Characterization of porous silicon carbide according to absorption and photo-luminescence spectra. *Semiconductors.* 2014. **48**. P. 1028–1030. https://doi.org/10.1134/S1063782614080041.
22. Fan J.Y., Wu X.L., Paul K. Chu. Low-dimensional SiC nanostructures: Fabrication, luminescence, and electrical properties. *Prog. Mater. Sci*. 2006. **51**. P. 983. https://doi.org/10.1016/j.pmatsci.2006.02.001.

23. Lee K.-H., Lee S.-K., Jeon K.-S. Photoluminescent properties of silicon carbide and porous silicon carbide after annealing. *Appl. Surf. Sci.* 2009. **255**. P. 4414–4420. https://doi.org/10.1016/j.apsusc.2008.11.047.
24. Rossi A.M., Ballarini V., Ferrero S., Giorgis F. Vibrational and emission properties of porous 6H-SiC. *Mater. Sci. Forum.* 2004. **457-460**. P. 1475–1478. https://doi.org/10.4028/www.scientific.net/MSF.457-460.1475.
25. Rittenhouse T.L., Bohn P.W., Hossain T.K. *et al*. Surface-state origin for the blueshifted emission in anodically etched porous silicon carbide. *J. Appl. Phys*. 2004. **95**. P. 490–496. https://doi.org/10.1063/1.1634369.
26. Matsumoto T., Takahashi J., Tamaki T. *et al*. Blue-green luminescence from porous silicon carbide. *Appl. Phys. Lett*. 1994. **64**. P. 226–228. https://doi.org/10.1063/1.111979.
27. Gavrilchenko I.V., Milovanov Y.S., Gryn S.V. *et al*. Spectral-luminescence properties of freestanding porous SiC layers. *J. Lumin*. 2021. **240**. P. 118466. https://doi.org/10.1016/j.jlumin.2021.118466.
28. Lu W., Tarekegne A.T., Ou Y. *et al*. Temperature-dependent photoluminescence properties of porous fluorescent SiC. *Sci. Rep.* 2019. **9**. P. 16333. https://doi.org/10.1038/s41598-019-52871-6.
29. Hassen F., M'Ghaieth R. *et al.* Morphological and optical characterization of porous silicon carbide. *Mater. Sci. Eng. C.* 2001. **15**. P. 113–115. https://doi.org/10.1016/S0928-493101.00252-1.
30. Kim S., Spanier J.E., Herman I.P. Optical transmission, photoluminescence, and Raman scattering of porous SiC prepared from *p*-type 6H SiC. *Jpn. J. Appl. Phys*. 2000. **39**. P. 5875–5878. https://doi.org/10.1143/JJAP.39.5875.
31. Lee K.-H., Du Y.-L., Lee T.-H. Photoluminescence and photoluminescence excitation from porous silicon carbide. *Bull. Korean Chem. Soc*. 2000. **21**. P. 769–773. https://doi.org/10.5012/bkcs.2000.21.8.769.
32. Chen Z.M., Ma J.P., Yu M.B. *et al*. Light induced luminescence centers in porous SiC prepared from nano-crystalline SiC grown on Si by hot filament chemical vapor deposition. *Mater. Sci. Eng.* 2000. **75**. P. 180–183. https://doi.org/10.1016/S0921-510700.00358-5.
33. Danishevskii M., Zamoryanskaya M.V., Sitnikova A.A. *et al*. TEM and cathodoluminescence studies of porous SiC. *Semicond. Sci. Technol*. 1998. **13**. P. 111.
34. Jessensky O., Müller F., Gösele U. Microstructure and photoluminescence of electrochemically etched porous SiC. *Thin Solid Films.* 1997. **297**. P. 224–228. https://doi.org/10.1016/S0040-609096.09419-9.
35. Konstantinov A.O., Henry A., Harris C.I., Janzen E. Photoluminescence studies of porous silicon carbide. *Appl. Phys. Lett*. 1995. **66**. P. 2250–2252. https://doi.org/10.1063/1.113182.
36. Bacherikov Yu.Yu., Dmitruk N.L., Konakova R.V. *et al*. Formation of titanium oxide films on the surface of porous silicon carbide. *Tech. Phys.* 2008. **53**. P. 1232–1235. https://doi.org/10.1134/S1063784208090168.
37. Bacherikov Y.Y., Konakova R.V., Lytvyn O.S. *et al.* Morphology and optical properties of titanium-doped porous silicon carbide layers. *Tech. Phys. Lett.* 2006. **32**, No 4. P. 140–142. https://doi.org/10.1134/S1063785006020167.
38. Nguyen H.A., Miyajima K., Itoh T. *et al*. The effect of the etching process on the morphology and photoluminescence of porous amorphous SiC. *Adv. Nat. Sci: Nanosci. Nanotechnol.* 2011. **2**. P. 025009. https://doi.org/10.1088/2043-6262/2/2/025009.
39. Alekseev S., Korytko D., Iazykov M. *et al*. Electrochemical synthesis of carbon fluorooxide nanoparticles from 3C-SiC substrates. *J. Phys. Chem*. C. 2015. **119**. P. 20503–20514. https://doi.org/10.1021/acs.jpcc.5b06524.
40. Wu X. L., Fan J. Y., Qiu T. *et al.* Experimental evidence for the quantum confinement effect in 3C-SiC nanocrystallites. *Phys. Rev. Lett*. 2005. **94**. 026102. https://doi.org/10.1103/PhysRevLett.94.026102.
41. Beke D., Szekrényes Z., Czigány Z. *et al*. Dominant luminescence is not due to quantum confinement in molecular-sized silicon carbide nanocrystals. *Nanoscale*. 2015. **7**. P. 10982–10988. https://doi.org/10.1039/C5NR01204J.
42. Lee H., Kim H., Seo H.S. *et al*. Comparative study of 4H-SiC epitaxial layers grown on 4 off-axis Si- and C-face substrates using bistrimethylsilylmethane precursor. *ECS J. Solid State Sci. Technol*. 2015. **4**. P. N89–N95. http://dx.doi.org/10.1149/2.0111508jss.
43. Kumari S., Kumar R., Agrawal P.R. *et al*. Fabrication of lightweight and porous silicon carbide foams as excellent microwave susceptor for heat generation. *Mater. Chem. Phys.* 2020. **253**. P. 123211. https://doi.org/10.1016/j.matchemphys.2020.123211.
44. Bachurina D.V., Murzaev R.T., Nazarov A.A. Relaxation of dislocation structures under ultrasonic influence. *Int. Journal of Solids and Structures*. 2019. **156–157**. P. 1–13. https://doi.org/10.1016/j.ijsolstr.2018.06.007.
45. Matare H.F. *Defect Electronics in Semiconductors.* New York, Wiley-Interscience, 1971.
46. Nowick A.S., Berry B.S. *Anelastic Relaxation in Crystalline Solids*. Academic Press, New York and London, 1972.
47. Zhou J., Xu W., You Z. *et al.* A new type of power energy for accelerating chemical reactions: The nature of a microwave-driving force for accelerating chemical reactions. *Sci. Rep.* 2016. **6**. P. 25149. https://doi.org/10.1038/srep25149.

Authors and CV

Olga B. Okhrimenko, defended his Doctoral Dissertation in Physics and Mathematics in 2010. Leading scientific collaborator at the V. Lashkaryov Institute of Semiconductor Physics. Authored over 150 publications, 1 patent, 1 monograph. The area of her scientific interests includes investigation of the patterns and physical mechanisms of formation and rearrangement of the defect-impurity system of the thin-film dielectric-semiconductor structures, depending on technology of preparation, composition of thin films, additional processing and introduction of buffer layers.
https://orcid.org/0000-0002-7611-4464

Yuriy Yu. Bacherikov defended his Doctoral Dissertation in Physics and Mathematics in 2010. Leading scientific collaborator at the V. Lashkaryov Institute of Semiconductor Physics. Authored over 300 publi-cations, 6 patents, 1 monograph. The area of his scientific interests includes physics and applications of wide-band semiconductor compounds and devices based on them. E-mail: yuyu@isp.kiev.ua;
https://orcid.org/0000-0002-9144-4592

Raisa V. Konakova, Professor, Doctor of Technical Sciences, Head of the Laboratory of Physical and Technological Problems of Solid State SHF Electronics at the V. Lashkaryov Institute of Semiconductor Physics. The area of scientific interests of Dr R.V. Konakova includes physics of metal-semiconductor junctions.
E-mail: konakova@isp.kiev.ua

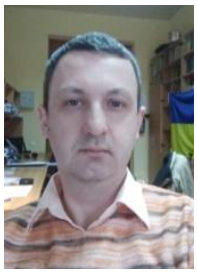

Oleksandr F. Kolomys, PhD in Physics and Mathematics. Senior Researcher at the Laboratory of Submicron Optical Spectroscopy, V. Lashkaryov Institute of Semiconductor Physics. Authored over 130 publications, 3 patents, 3 chapters of textbooks. The area of his scientific interests includes Raman and luminescent microanalysis of light emitting properties, structure, composition, electronic and phonon excitations in solids, physical and chemical properties of semiconductors, chemicals and nanostructures for modern micro-, nano- and optoelectronics with submicron spatial resolution.
E-mail: olkolomys@gmail.com;
https://orcid.org/0000-0002-1902-4075

Viktor V. Strelchuk, Professor, Doctor of Sciences in Physics and Mathematics, Head of Optical Submicron Spectroscopy Laboratory at the V. Lashkaryov Institute of Semiconductor Physics. Field of research: physics of semiconductors, Raman and photoluminescence spectroscopy of semiconductors, nanostructures and nanoscale materials. He is the author of more than 100 scientific publications and technical patents.
E-mail: viktor.strelchuk@ccu-semicond.net;
https://orcid.org/0000-0002-6894-1742

Authors' contributions

Okhrimenko O.B.: key ideas, conceptualization, investigation, writing – original draft, supervision.
Bacherikov Yu.Yu.: key ideas, conceptualization, investigation, writing – review & editing.
Kolomys O.F.: performed experiments of Raman and luminescent microanalysis, analyzing the data.
Strelchuk V.V.: validation, investigation Raman and luminescent experimental data.
Konakova R.V.: administrator.

Перерозподіл центрів випромінювальної рекомбінації в структурах SiC/por-SiC та SiC/por-SiC/Er_2O_3 за нетепловою дією мікрохвильового випромінювання

О.Б. Охріменко, Ю.Ю. Бачеріков, О.Ф. Коломис, В.В. Стрельчук, Р.В. Конакова

Анотація. У даній роботі розглянуто вплив короткочасної нетеплової дії мікрохвильового випромінювання на фотолюмінесцентні характеристики структур SiC/por-SiC/Er_2O_3 та SiC/por-SiC. Аналіз спектрів фотолюмінесценції цих структур при збудженні випромінюванням з енергією, меншою за ширину забороненої зони кристалічної підкладки 4H-SiC, показав, що короткочасна дія мікрохвильового випромінювання приводить до перерозподілу центрів випромінювальної рекомбінації, що зумовлено поверхневими станами у шарі por-SiC.

Ключові слова: нетеплова мікрохвильова дія, буферний пористий шар, фотолюмінесценція, комбінаційне розсіювання, карбід кремнію.